

# Silibinin exhibits anti-tumor effects in a breast cancer stem cell model by targeting stemness and induction of differentiation and apoptosis

Javad Firouzi<sup>1,2,3</sup>, Fattah Sotoodehnejadnematalahi<sup>4</sup>, Alireza Shokouhifar<sup>3</sup>, Mahsa Rahimi<sup>3</sup>, Niloufar Sodeifi<sup>5</sup>, Parisa Sahranavardfar<sup>3</sup>, Masoumeh Azimi<sup>3</sup>, Ehsan Janzamin<sup>3</sup>, Majid Safa<sup>1,2,6</sup>, Marzieh Ebrahimi<sup>3\*</sup>

<sup>1</sup>Department of Tissue Engineering & Regenerative Medicine, Faculty of Advanced Technologies in Medicine, Iran University of Medical Sciences, Tehran, Iran

<sup>2</sup>Cellular and Molecular Research Centre, Iran University of Medical Sciences, Tehran, Iran

<sup>3</sup>Department of Stem Cells and Developmental Biology, Cell Science Research Center, Royan Institute for Stem Cell Biology and Technology, ACECR, Tehran 16635-148

<sup>4</sup>Department of Biology, School of Basic Science, Science and Research Branch, Islamic Azad University, 1477893855

<sup>5</sup>Department of Pathology, Reproductive Biomedicine Research Center, Royan Institute for Reproductive Biomedicine, ACECR, Tehran 16635-148, Iran

<sup>6</sup>Department of Hematology, Faculty of Allied Medicine, Iran University of Medical Sciences, Tehran, Iran

## Article Info



### Article Type:

Original Article

### Article History:

Received: 9 Aug. 2020

Revised: 27 Aug. 2021

Accepted: 18 Sep. 2021

ePublished: 17 Aug. 2022

### Keywords:

Breast cancer stem cells,  
 Silibinin,  
 Mammospheres,  
 Epithelial to mesenchymal  
 transition

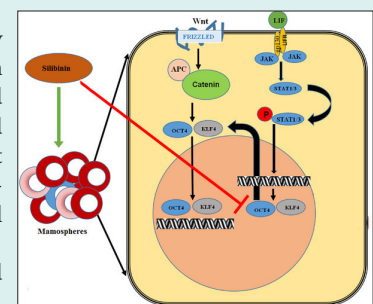
## Abstract

**Introduction:** Malignant breast cancer (BC) frequently contains a rare population of cells called cancer stem cells which underlie tumor relapse and metastasis, and targeting these cells may improve treatment options and outcomes for patients with BC. The aim of the present study was to determine the effect of silibinin on the self-renewal capacity, tumorigenicity, and metastatic potential of mammospheres.

**Methods:** The effect of silibinin on viability and proliferation of MCF-7, MDA-MB-231 mammospheres, and MDA-MB-468 cell aggregation was determined after 72-120 hours of treatment. Colony and sphere formation ability, and the expression of stemness, differentiation, and epithelial-mesenchymal-transition (EMT)-associated genes were assessed by reverse transcription-quantitative polymerase chain reaction (qRT-PCR) in mammospheres treated with an IC<sub>50</sub> dose of silibinin. Additionally, the antitumor capacity of silibinin was assessed *in vivo*, in mice.

**Results:** The results of the present study showed that silibinin decreased the viability of all mammospheres derived from MCF-7, MDA-MB-231, and MDA-MB-468 cell aggregation in a dose-dependent manner. Colony and sphere-forming ability, as well as the expression of genes associated with EMT were reduced in mammospheres treated with silibinin. Additionally, the expression of genes associated with stemness and metastasis was also decreased and the expression of genes associated with differentiation were increased. Intra-tumoral injection of 2 mg/kg silibinin decreased tumor volumes in mice by 2.8 fold.

**Conclusion:** The present study demonstrated that silibinin may have exerted its anti-tumor effects in BC by targeting the BC stem cells, reducing the tumorigenicity and metastasis. Therefore, silibinin may be a potential adjuvant for treatment of BC.



## Introduction

Breast cancer (BC) is the second leading cause of cancer-associated deaths in women worldwide,<sup>1</sup> and is often composed of a collection of different cell populations with varying properties.<sup>2</sup> Frequently, a small population of tumor cells with self-renewal capacity and resistance

to commonly used therapeutics remain in patients who have been treated with conventional therapies, and these remaining cells are responsible for tumor growth, expansion, and metastasis.<sup>3-5</sup> Therefore, targeting and eliminating these tumor stem cells at the same time as the rest of the tumor may reduce relapse rates. However,



\*Corresponding author: Marzieh Ebrahimi, Email: mebrahimi@royaninstitute.org



© 2022 The Author(s). This work is published by BioImpacts as an open access article distributed under the terms of the Creative Commons Attribution Non-Commercial License (<http://creativecommons.org/licenses/by-nc/4.0/>). Non-commercial uses of the work are permitted, provided the original work is properly cited.

developing a suitable model of cancer stem cells (CSCs) to be used in pharmacological studies remains a challenge. The majority of chemotherapeutics are initially tested two-dimensionally on a monolayer of tumor specific sorted stem cells based on their cell surface markers,<sup>6</sup> and this does not accurately reflect the tumor environment in patients. Another commonly used method for studying potential chemotherapeutics are xenograft mouse models or patient-derived xenograft models which are expensive and time-consuming, and numerous ethical concerns need to be taken into consideration, which may limit the scope of the studies.<sup>7</sup> Three dimensional (3D) tumor cell culture provides a more accurate representation of the tumor environment and is more likely to retain or replicate the proper signaling pathways, cell-cell interactions, and adhesions present *in vivo*.<sup>8</sup> Conclusions drawn from 3D tumor cultures may also be accurate as the exposure to drug treatments, stress, and oxygenation will be more representative of the tumor environment.<sup>9</sup> Additionally, development of tumor spheres in serum-free medium with reduced cell attachment properties may be useful in enriching CSCs. The aim of the present study was to use mammosphere models to investigate CSC richness, and to imitate tumor masses *in vitro*.

Over the past two decades, silymarin and its primary component silibinin, have been demonstrated to possess anticancer effects,<sup>10</sup> by targeting multiple events associated with tumor growth, including apoptosis,<sup>11,12</sup> cell cycle arrest,<sup>12,13</sup> inflammation,<sup>14</sup> angiogenesis,<sup>15</sup> cancer cell metabolism,<sup>16,17</sup> and invasion and metastasis,<sup>18-20</sup> with little to no toxic effects. Furthermore, silibinin combined with metformin enhanced the antiproliferative effects of metformin on BC cells through downregulation of cyclin D1 and hTERT gene expression,<sup>21</sup> and also enhanced the apoptotic effects of paclitaxel toxicity on various human gastric cancer cell lines.<sup>22</sup> Previous studies have demonstrated the potential of silibinin to target stemness and metastasis in bladder cancer through inhibition of the  $\beta$ -catenin/ZEB1 signaling pathway,<sup>23</sup> suppression of nuclear factor- $\kappa$ B activation in breast carcinoma,<sup>24</sup> by modulating interleukin 4/6-mediated survival signals in colon CSC-enriched spheroids.<sup>25</sup> Additionally, a combination of silibinin and spheroids reduced the phosphorylation of STAT3/ERK/AKT in CSCs of hepatocellular carcinoma.<sup>26</sup> Our previous study also showed the potential of silibinin to reduce stemness and induce apoptosis in 2D and 3D models of the MDA-MB-468 breast carcinoma cell line.<sup>27</sup> However, its effect on BC stem cells is unclear *in vitro* and *in vivo*. In the present study, mammospheres were used as a breast cancer stem cell (BCSC) model to determine the effect of silibinin on self-renewal capacity and the invasive potential. Furthermore, the effects of silibinin on tumor growth *in vivo* were evaluated. The results of the present study may improve our understanding of the mechanisms underlying the anti-cancer effects of silibinin in BC as well as improving our ability to specifically target the BC stem cells.

## Materials and Methods

### Cell lines and culture conditions

In the present study four BC cell lines were used: MCF-7 as a ER<sup>+</sup>, PR<sup>+</sup> cell line; MDA-MB-231 cells, a poorly differentiated triple-negative BC (TNBC) cell line; MDA-MB-468 as a TNBC; and epithelial Mouse BC 4T1 cells, a 6-thioguanine resistant cell line (the passage number of all the cell lines cultures was three). All the human cell lines were purchased from the Iranian Biological Resource Center and the 4T1 cell line was purchased from Pasteur Institute of Iran. Human cell lines were cultivated in DMEM and 4T1 cells were cultured in RPMI-1640 supplemented with 2 mmol/L L-glutamine, 100 U/mL penicillin, 100  $\mu$ g/mL streptomycin, non-essential amino acid, and 10% FBS (all purchased from Invitrogen; Thermo Fisher Scientific, Inc.). Cells were incubated with 5% CO<sub>2</sub> at 37°C. Trypsin/EDTA (Invitrogen; Thermo Fisher Scientific, Inc.) was used to harvest the cells.

### Mammosphere culture

The mammospheres were formed using an anchorage-independent method. Flat-bottom 96-well plates and T25 flasks were coated with 12 mg/mL poly 2-hydroxyethyl methacrylate (Poly-HEMA; Sigma-Aldrich; Merck KGaA) in 95% ethanol and washed once with PBS before cell seeding. A total of  $9 \times 10^4$  viable cells were transferred into a non-adherent T25 flask in 5 mL sphere medium including DMEM supplemented with basic fibroblast growth factor (bFGF; Royan Institute), 20 ng/mL epithelial growth factor (EGF; Royan Institute), and 2% B27 (Thermo Fisher Scientific, Inc), Fresh EGF, bFGF, and B27 were added every 2 days.

### Cell viability and proliferation assay

The CellTiter 96 Aqueous One Solution Cell Proliferation assay (Promega Corporation), which includes MTS was used according to the manufacturer's protocol to evaluate cell viability. For assessment of cell viability,  $1.5 \times 10^3$  cells/well were seeded into poly-HEMA-coated 96-well plates and cultivated in sphere medium for 96 hours to induce mammosphere formation. Subsequently, silibinin (Sigma-Aldrich; Merck KGaA) was dissolved in ethanol according to the manufacturer's protocol, added to media to a final concentration of 0-1,600  $\mu$ mol, and incubated for 72 hours at 37°C with 5% CO<sub>2</sub>. For the cell proliferation assay,  $2 \times 10^3$  mammosphere derived cells per well from the control (treated with ethanol alone) and the test group (treated with an IC<sub>50</sub> dose of silibinin) were seeded in flat-bottom 96-well plates and incubated at 37°C with 5% CO<sub>2</sub> for 24, 48, 72, 96, and 120 hours. In both experiments, MTS was added to each well at the end of incubation time and further incubated for another 3 hours. Subsequently, 100  $\mu$ L media from every well were transferred to a new flat-bottom 96-well plate and the optical density of the culture medium was measured at 490 nm using a microplate reader (Bio-Tek Instruments, Ltd.). Viability of cells in the

mammospheres was calculated as a percentage as follows: (Average absorbance in the silibinin treated group/average absorbance in the control group)  $\times$  100. Viability assays were performed in triplicate.

### Clonogenic assay

Mammospheres treated with an  $IC_{50}$  dose of silibinin for 72 hours were washed and dissociated using trypsin/EDTA. A total of 200 viable cells from both the control and treated groups were transferred into each well of a 6-well plate containing 2 mL supplemented DMEM. After 12 days of culturing, the medium was discarded, cells were washed with calcium and magnesium-free PBS, and fixed with 4% paraformaldehyde at 4°C for 45 minutes. Colonies were stained with 200  $\mu$ L 0.05% crystal violet for 5 minutes at room temperature (RT) and counted using an inverted light microscope at  $\times$ 10 magnification. All results were normalized to the ethanol group. A 6-well plate was used for each replicate (two wells per a cell line) and 20–40 colonies were counted for each condition. At least three biological replicates were performed. For size analysis, all colonies in all nine experiments were analyzed using an inverted light microscope at  $\times$ 10 magnification and cellSens Standard software version 1.5 (CellSens B.V.). Clonogenicity was calculated as follows: (Average number of colonies formed/number of cells seeded)  $\times$  100.

### Mammosphere formation efficiency assay

Mammospheres treated with an  $IC_{50}$  dose of silibinin for 72 hours were washed and cells were dissociated using trypsin/EDTA. A total of  $3 \times 10^4$  viable cells/well were plated in poly-HEMA-coated 6-well plates containing 2 mL sphere medium. Fresh EGF, bFGF, and B27 were added every 3 days. Mammospheres with diameters of 150–400  $\mu$ m were counted after 7 days of culture. The mean diameter (d) of the mammospheres was determined using the following equation:  $d = (axb)^{1/2}$ , where a and b are the orthogonal diameters of the spheroid.<sup>28</sup>

### Invasion and migration assay

Invasion and migration assays were performed in 24-well plates with 8.0  $\mu$ m pore Transwell inserts (EMD Millipore). In order to investigate invasive ability, filters were pre-coated with 60  $\mu$ L of diluted Matrigel (0.5 mg/mL; Sigma-Aldrich; Merck KGaA) for 12 hours. Uncoated filters were used for the migration assays. A total of  $2.5 \times 10^4$  cells derived from treated (72 hours with an  $IC_{50}$  dose of silibinin) and control mammospheres in 200  $\mu$ L serum-free culture medium was added to the filter inserts. Each filter was placed in the lower chamber with 600  $\mu$ L culture medium containing 10% FBS. Filters were incubated at 37°C with 5%  $CO_2$  for 12 hours. The cells which remained on the inside of the filter were removed using a cotton swab and cells attached to the bottom surface of filters were fixed with 4% paraformaldehyde at 4°C for 45 minutes, and subsequently stained with a 0.5%

crystal violet for 5 minutes at RT. The number of attached cells on the bottom surface of the filter was counted in 10 randomly selected fields using inverted light microscope at  $\times$ 20 magnification, and all counts were normalized to the control.

### Flow cytometry analysis

The levels of the CD44<sup>+</sup>, CD24<sup>-</sup>, and CD133<sup>+</sup> cells in each group were evaluated using flow cytometry with a fluorescein isothiocyanate (FITC)-conjugated CD44 antibody (cat. no. 347943; BD Biosciences), phycoerythrin (PE)-conjugated CD24 antibody (cat. no. 555428; BD Biosciences), and a PE-conjugated CD133 antibody (cat. no. 12-1331-82; eBioscience; Thermo Fisher Scientific, Inc.). Mouse immunoglobulin (Ig)G2a-FITC (cat. no. 555573; BD Biosciences), mouse IgG2a-PE (cat. no. 554648; BD Biosciences), and mouse IgG1K-PE (cat. no. 12-4714-42; eBiosciences Thermo Fisher Scientific, Inc.) were used as the isotype controls (all of antibodies diluted at 1:100 ratio). Cells were incubated with antibodies at 4°C for 45 minutes and analyzed using FACSCalibur™ (Becton Dickinson). The raw data were analyzed using Flowing Software version 2.5.0 (Perttu Terho).

### Reverse transcription-quantitative (q-RT) PCR

Total RNA was extracted from mammospheres in control and treated groups using TRIzol<sup>®</sup> reagent (Sigma-Aldrich; Merck KGaA) and any DNA was digested using RNase free DNase I (Takara Bio, Inc.) according to the manufacturer's protocol. cDNA was generated using RevertAid H Minus First Strand cDNA kit (Fermentas; Thermo Fisher Scientific, Inc.) according to the manufacturer's instructions. The thermocycling conditions for qRT-PCR were: 95°C for 15 seconds and 60°C for 60 seconds for 40 cycles. The expression of the stemness-associated genes *OCT4*, *c-MYC*, *KLF4*, *SOX2*, *CK8*, *CK18*, *CK19*, *NANOG*, *CDH1*, *CDH2*, *SNAIL1*, *SNAIL2*, *TWIST1*, *TWIST2*, and *ZEB1* was assessed using a Rotor Gene 6000 Real-Time PCR machine (Qiagen China Co., Ltd.) and analyzed using Rotor Gene 6000 version 1.7 (Qiagen China Co., Ltd.). SYBR Green PCR Master mix (Applied Biosystems) was used for qPCR according to the manufacturer's protocol. The list of human-specific primers used, and their sequences are presented in Table 1. Melting curve analysis from 65–95°C was performed, the results were normalized to GAPDH, and data were analyzed using the  $2^{-\Delta\Delta Cq}$  method.<sup>29</sup>

### Generation of a BC mouse model

All studies *in vivo* were performed according to the guidelines for animal care established by the Royan Institute's Animal Care Committee and approved by the Institutional Review Board and Ethics Committee of the Royan Institute. A total of  $1 \times 10^6$  4T1 cells in 100  $\mu$ L Matrigel were injected in the flank of inbred females Balb-C mice (n: 15 mice, weight: 18–21 g, Supplier:

**Table 1.** Primer sequences used for reverse transcription-quantitative PCR

Primer	Sequence	Length, bp	NCBI accession number
SOX2	F, 5'-GGGAAATGGAAGGGTGCAAAAGAGG-3' R, 5'-TTGCGTGAGTGTGGATGGGATTGGTG-3'	151	NM_003106.3
Klf4	F, 5'-ATTACCAAGAGCTCATGCCA-3' R, 5'-CCTTGAGATGGGAAGCTCTTTG-3'	150	NM_004235.4
NANOG	F, 5'-AAAGAATCTTCACCTATGCC-3' R, 5'-GAAGGAAGAGGAGAGACAGT-3'	110	NM_024865.2
OCT4	F, 5'-CTGGGTTGATCCTCGGACCT-3' R, 5'-CACAGAACTCATACTGGCGGG-3'	128	NM_002701.4
c-MYC	F, 5'-ACACATCAGCACAACACTACG-3' R, 5'-CGCCTCTTGACATTCTCC-3'	140	NM_002467
TWIST1	F, 5'-CCAGGTACATCGACTTCCTC-3' R, 5'-TCGTGAGCCACATAGCTG-3'	85	NM_000474.3
TWIST2	F, 5'-GCGCAAGTGGAAATGGGATG-3' R, 5'-CGGGTCTTCTGTCCGATGC-3'	128	NM_001271893.4
CDH1	F, 5'-CAGGAGTCATCAGTGTGGT-3' R, 5'-GGAGGATTATCGTTGGTGTGAG-3'	150	NM_004360.3
CDH2	F, 5'-GCCCAAGACAAAGAGACCC-3' R, 5'-CTGCTGACTCCTCACTGAC-3'	93	NM_001792.3
SNAIL1	F, 5'-CCAGAGTTTACCTTCCAGCA-3' R, 5'-GATGAGCATTGGCAGCGA-3'	101	NM_005985.3
SNAIL2	F, 5'-AACTACAGCGAACTGGACAC-3' R, 5'-GGATCTCTGGTTGTGGTATGAC-3'	90	NM_003068.3
$\beta$ -actin	F, 5'-TCCCTGGAGAAGAGCTACG-3' R, 5'-GTAGTTTCGTGGATGCCACA-3'	131	NM_001101.3
ZEB1	F, 5'-GAGGATGACACAGGAAAGGA-3' R, 5'-CAGCAGTGTCTTGTGTGT-3'	163	NM_0011281282
NOTCH	F, 5'-CAGACCACACCCAGTA-3' R, 5'-GGCAACGTCAACACCTT-3'	114	NM_017617
CD133	F, 5'-GCATCCATCAAGTGAACGT-3' R, 5'-GGTTTGCGGTTGTAAGTCTGT-3'	199	NM_001145852.1
CK8	F, 5'-CAGATCAAGACCCTCAACAAC-3' R, 5'-CACTTGGTCTCCAGCATCTT-3'	89	NM_001256293.1
CK18	F, 5'-GCGAGGACTTTAATCTTGGTG-3' R, 5'-CTTTGGTGTCAATTGGTC CAG-3'	120	NM_199187.1
CK19	F, 5'-GCGACTACAGCCACTACTACA-3' R, 5'-TGGTTCGGAAGTCATCTGC-3'	129	NM_002276.4

Royan Institute). The mice developed tumors 7 days after injection of cells, at which point, tumor-bearing mice were divided into four groups randomly: Control, solvent, 10X, and 20X. Each group contained three mice. The control group did not receive any treatment, the solvent group received ethanol, the 10X group received 1 mg/kg silibinin (10 fold dose of *in vitro*), and the 20X group received 2 mg/kg silibinin (20 fold dose of *in vitro*). The solvent and silibinin were injected directly into the tumor. Injections of solvent and silibinin were performed every 72 hours after the tumor diameter reached 4-6 mm, and tumor size was measured daily with calipers. All mice were sacrificed at day 20 post-treatment and tumors were removed for pathological and immunohistochemical evaluation.

#### **Hematoxylin and eosin (H&E) staining and immunohistochemistry**

Tumor tissues were removed, fixed in 10% formalin at RT for 72 hours, and embedded into paraffin blocks. Tissues were sectioned (5  $\mu$ m thickness), deparaffinized using xylol, and stained using H&E at RT for 45 minutes. The rate

of mitosis, pleomorphism, inflammation, karyorrhexis, and desmoplasia per a field of view was evaluated by an independent pathologist at a magnification of  $\times 400$ . For Immunohistochemistry evaluation, the slides were deparaffinized and rehydrated in a decreasing series of ethanol solutions (two incubations in 100% for 3 minutes each, 96% for 3 minutes, 70% for 3 minutes, and distilled water for 3 minutes). Slides were incubated in 3% hydrogen peroxide in methanol for 20 minutes at room temperature to inhibit endogenous peroxidase activity. Citrate buffer (pH = 6.0) and autoclaving for 10 minutes at 120°C with pressure were used for antigen retrieval. After the slides had cooled, they were washed in Tris-buffered saline (TBS). The sections were incubated at 4°C overnight with anti-human  $\alpha$ -SMA antibody recognizing the cytoplasmic SMA which surrounded the vessels (1:200; Cat. No. ab7817; Abcam). The sections were washed the following day and incubated with the horseradish peroxidase-conjugated anti-mouse secondary antibody diluted in PBS (1:500; Cat. No. ab205719; Abcam) for 60 minutes at RT. The sections were then stained with 3, 3'-diaminobenzidine

(Dako) substrate as the chromogen for two minutes in the dark and at room temperature. Subsequently, the sections were counterstained with hematoxylin (Dako; Agilent Technologies, Inc.). All images were captured on an Olympus BX51 fluorescence microscope.

### Western blot analysis

A total of 35  $\mu\text{g}$  protein was extracted from treated and non-treated mammospheres using Q Proteom Mammalian Protein Prep kit (Cat. No. 37901; Thermo Fisher Scientific, Inc.), preheated at 100°C for 3 minutes in a reducing sample buffer containing 50 mM Tris-Cl (pH 6.8), 2% SDS, 10% glycerol, 0.1% Bromophenol blue, and 100 mM  $\beta$ -Mercaptoethanol, were loaded on a 10% SDS gel and resolved using SDS-PAGE. Protein concentration was measured using a protein assay kit (cat. no. 23225; Thermo Fisher Scientific, Inc.). Proteins were subsequently transferred to a PVDF membrane (Whatman Plc; GE Healthcare Life Sciences). After transfer, membranes were blocked with 5% BSA in TBS at RT for 60 minutes, followed by an overnight incubation with either anti-phospho-STAT3 or anti-GAPDH (Sigma Aldrich; Merck KGaA; cat. no. ZRB1004) in 5% BSA in TBS at 4°C (both 1:1,000). After washing with TBS containing 0.1% Tween 20, the membranes were incubated with horseradish peroxidase-conjugated secondary antibody (Abcam; cat. no. ab205719; 1:7,000) in 5% skimmed milk powder in TBS for 2 hours at RT. Protein bands were visualized using Pierce enhanced chemiluminescence western blotting substrate (Pierce; Thermo Fisher Scientific, Inc.; cat. no. 32106) and western blotting was performed three times for each experiment independently.

### Search Tool for Interactions of Chemicals (STITCH)

STITCH (version 5; stitch.embl.de/) is a database of known and predicted interactions between chemicals and proteins based on computational predictions and established interactions in other organisms, and from interactions aggregated from other (primary) databases. The interactions include direct (physical) and indirect (functional) associations. The STITCH database was used and the experimentally validated genes and silibinin were searched. Using the STITCH database, interactions between silibinin and genes that were validated in the present study were evaluated.

### Statistical analysis

Student's *t* test, and one-way ANOVA or a two-way ANOVA were used for comparing the means of two independent groups, comparing more than 2 independent groups or analyzing and comparing the means of dependent groups, respectively. All experiments were performed in triplicate, and data were presented as the mean  $\pm$  standard deviation.  $P \leq 0.05$  was considered to indicate a statistically significant difference. Statistical analysis was performed using GraphPad Prism version 5 (GraphPad Software, Inc.).

## Results

### Silibinin reduces the viability and growth rate of mammospheres

To determine the cytotoxic effect of silibinin on mammospheres, mammospheres were treated with different concentrations of silibinin for 72 hours. The results showed that silibinin significantly reduced cell viability of

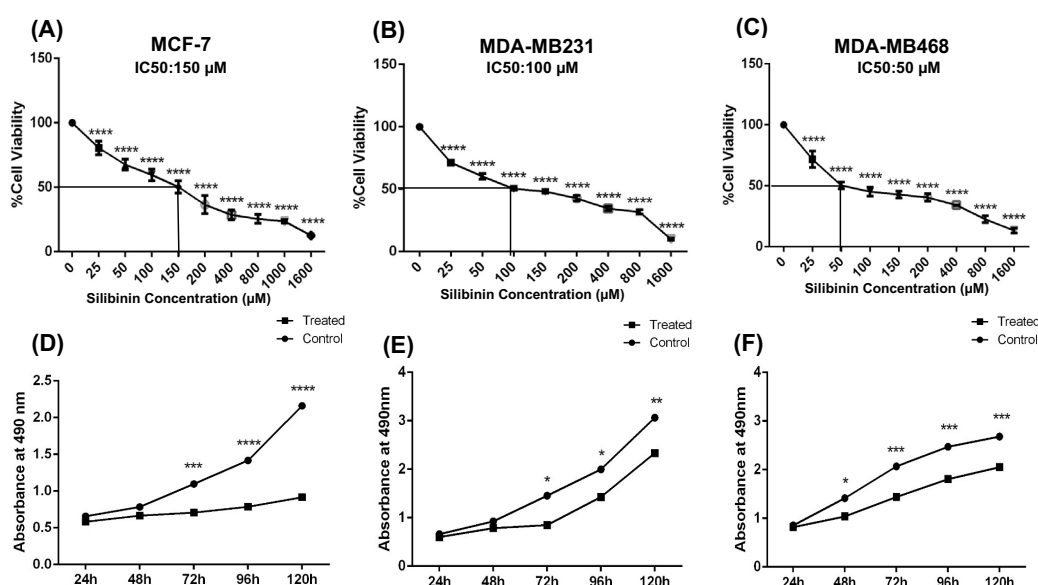


**Fig. 1.** Silibinin reduces the viability and proliferation of mammospheres. Mammospheres derived from breast cancer lines were treated with 0-1600  $\mu\text{M}$  of silibinin for 72 hours and the viability of cells were assessed. The  $\text{IC}_{50}$  doses of silibinin were determined to be (A) MCF-7, 150  $\mu\text{M}$ ; (B) MDA-MB-231, 100  $\mu\text{M}$ ; Mammospheres and (C) MDA-MB-468, 50  $\mu\text{M}$ . (D-F) aggregated cells were treated with the respective  $\text{IC}_{50}$  doses and proliferation was assessed in cells treated for 24, 48, 72, 96 and 120 hours. Silibinin-treated cells exhibited significantly reduced proliferation compared with the respective controls at the same time point. Data are presented as the mean + standard deviation of three different biological repeats. \* $P < 0.05$ , \*\* $P < 0.01$ , \*\*\* $P < 0.001$ , \*\*\*\* $P < 0.0001$ .

mammospheres in a dose-dependent manner (Fig. 1A-C). The IC<sub>50</sub> dose of silibinin was determined to be 150 μM, 100 μM, and 50 μM for MCF-7, MDA-MB-231 derived-mammospheres, and MDA-MB-468 cell aggregation, respectively. Furthermore, mammospheres treated with the IC<sub>50</sub> doses of silibinin, exhibited significantly reduced proliferation 120 hours post-treatment ( $P < 0.001$ ; Fig.

1D-F). Mammospheres derived from MCF-7 cells were presented with the largest reduction in mammosphere growth when treated with silibinin.

**Silibinin reduces stemness properties and promotes differentiation of cells in mammospheres**

An important characteristic of CSCs is a capacity to self-

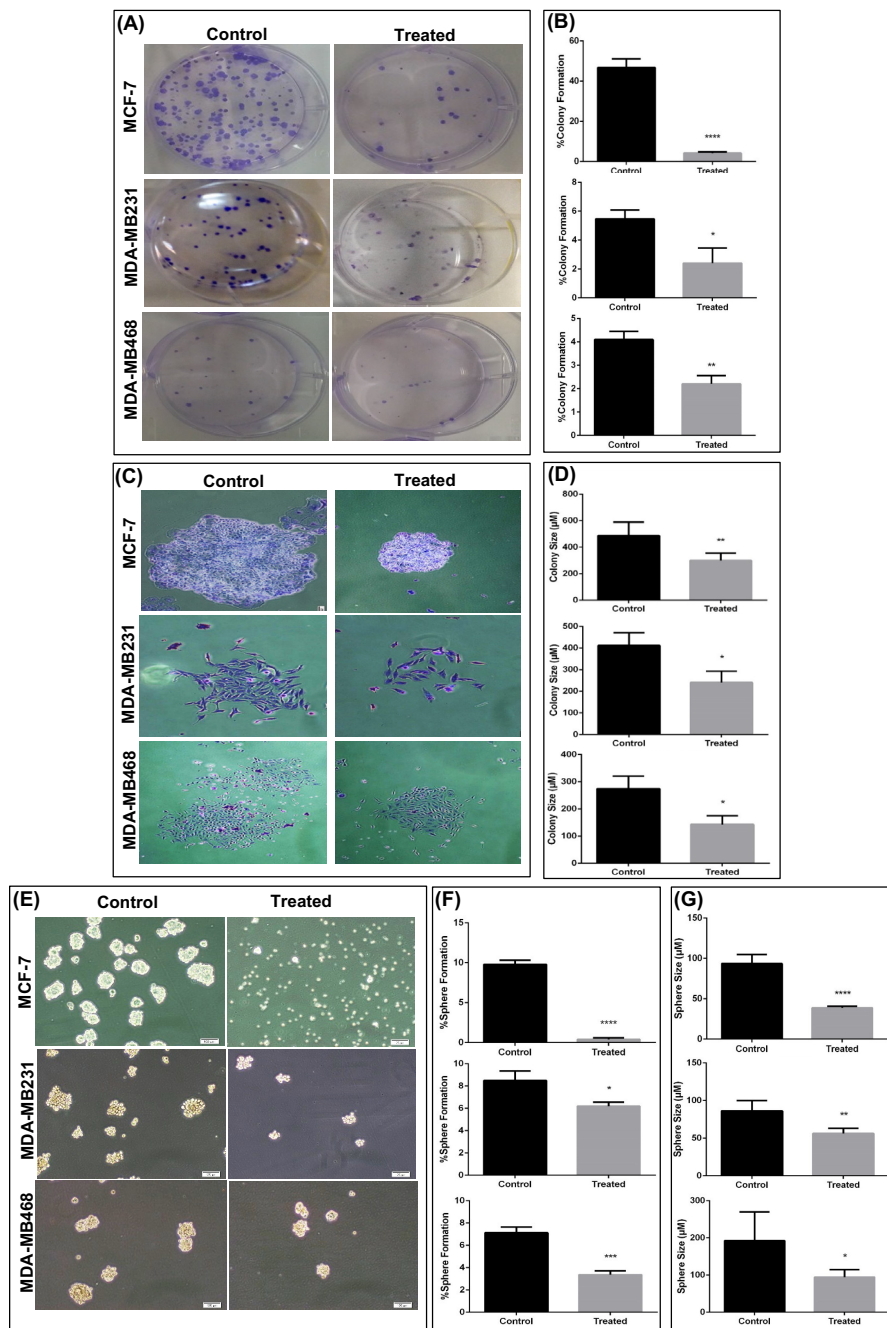


**Fig. 2.** Colony and sphere formation ability is reduced in mammospheres treated with silibinin. (A) Representative images of colony formation in BC cell lines treated with control or the respective IC<sub>50</sub> dose for 72 hours. (B) Percentage colony formation was calculated by counting the number of colonies in different cell lines and treatments. The number of colonies formed was significantly lower in the treated cells compared with the respective control. (C) Representative images of staining of a single colony with crystal violet. Magnification, x20. (D) The size of colonies were significantly smaller in cells treated with silibinin compared with the respective control. (E) Morphology of mammospheres and cell aggregation after 7 days of culture. (F) Sphere formation was significantly reduced in MCF-7 and MDA-MB-231 cell lines treated with silibinin compared with the respective untreated cells. The reduction in sphere formation was the largest in the MCF-7 cells. (G) Sphere size was significantly reduced in the cells treated with silibinin compared with the respective untreated cells. Data are presented as the mean + standard deviation of at least three biological repeats. \* $P < 0.05$ , \*\* $P < 0.01$ , \*\*\* $P < 0.001$ , \*\*\*\* $P < 0.0001$ . BC, breast cancer.

renew. To determine whether MCF-7, MDA-MB-231, and MDA-MB-468 cells exhibited this capacity *in vitro*, colony and sphere formation assays were used. In the colony formation assay, CSCs, progenitors, and fully differentiated cells propagated and created colonies with special characteristics. In the sphere formation assay, CSCs were the only cells which grew in serum-free medium on a non-adhesive surface.<sup>27,30,31</sup> There was a significant reduction in the number of colonies and colony size when mammospheres were treated with silibinin (Fig. 2A-D). Additionally, MCF-7-mammospheres treated with silibinin did not form spheroids, and MDA-MB-231-

mammosphere and MDA-MB-468-cell aggregation formed significantly fewer (Fig. 2E and F) and smaller spheroids (Fig. 2G). The effect of silibinin on spheroid formation was most prominent in MCF-7-mammospheres compared with the other cells.

Based on the above results, the expression of stemness-associated genes, including *OCT4*, *c-MYC*, *KLF4*, and *SOX2*, and the differentiation-associated cyto keratin genes including *CK8*, *CK18*, and *CK19* in mammospheres following treatment with silibinin was assessed. In treated mammospheres, expression of all the stemness-associated genes were all significantly downregulated

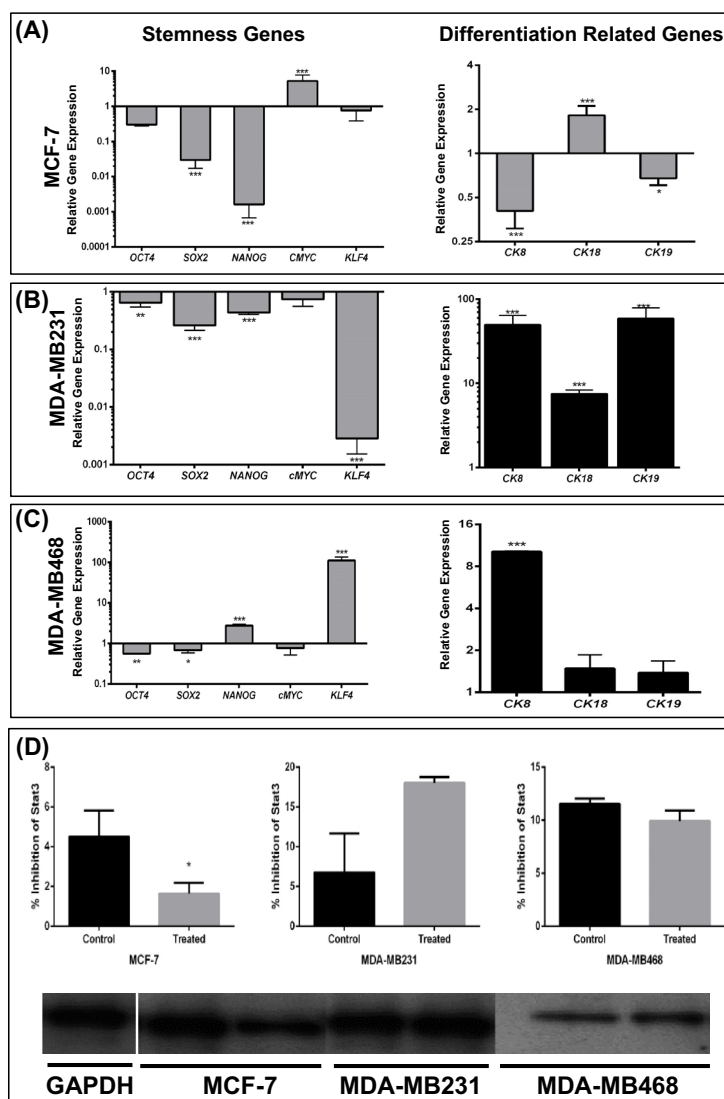


**Fig. 3.** Silibinin modulates the expression of stemness and epithelial-associated cyto keratin genes in derived -mammospheres and aggregated cells. (A) mRNA expression levels of *OCT4*, *SOX2*, and *KLF4* were reduced 2.4, 7.2, and 4.8 fold in treated MCF-7 mammospheres, respectively, and *c-MYC* was upregulated 7.4 fold in treated MCF-7 mammospheres. Expression of two differentiation-associated genes, *CK8* and *CK19*, were significantly downregulated whereas *CK18* was significantly upregulated. (B) Expression of stemness associated genes were all downregulated and all changes were determined to be significant except for *c-Myc*. All differentiation-associated genes were significantly upregulated in treated MDA-MB-231 cells. (C) In the MDA-MB-468 cells, expression of certain stemness-associated genes were upregulated whereas others were downregulated. *NANOG* and *KLF4* exhibited the largest changes in expression and both were upregulated. *c-MYC* expression was not significantly different. Expression of *CK8* was significantly increased whereas expression of *CK18* and *CK19* was not determined to be significantly different. GAPDH was used as the internal control. (D) Western blot analysis revealed that p-STAT3 protein expression was significantly reduced in the treated MCF-7 mammospheres and was not significantly changed in the other cell lines when treated with silibinin. However, the reduction in p-STAT3 may be the result of a reduction in total STAT3 expression which was not assessed. Data are presented as the mean  $\pm$  standard deviation of three biological repeats.  $^{*}P < 0.01$ ,  $^{***}P < 0.001$ ,  $^{****}P < 0.0001$ . *p*-, phospho; OD, optical density.

except for *c-MYC* in MCF-7-mammospheres, and *NANOG* and *KLF4* in MDA-MB-468 mammospheres (Fig. 3A-C). This reduction was accompanied with the overexpression of differentiation-associated genes in treated mammospheres derived from MDA-MB-231 and MDA-MB-468 (Fig. 3B and C). *CK18* was upregulated in treated MCF-7- mammospheres (Fig. 3A). The STAT3 pathway is an active signaling pathway in tumors which activates and enhances cell proliferation,<sup>28,32</sup> and activity of this pathway has been suggested to be increased in BCSCs.<sup>33,34</sup> As shown in Fig. 3D, silibinin significantly reduced the levels of Stat3 phosphorylation at tyrosine 705 in MCF-7-mammospheres, although this was not altered in mammospheres based on the other two cell lines. However, it was not possible to measure the expression levels of total Stat3, thus it cannot be stated with certainty, whether the total levels of Stat3 were reduced or phosphorylation of Stat3 was reduced.

Subsequently, the expression levels of surface markers associated with BCSCs, including CD44<sup>+</sup>/CD24<sup>-</sup><sup>35</sup> and CD133<sup>+</sup>CD44<sup>+</sup><sup>36,37</sup> following silibinin treatment were assessed. CD44 is a membrane glycoprotein which acts as a receptor for hyaluronic acid, and participates in cell adhesion migration and metastasis.<sup>38,39</sup> However, CD24 as an adhesion molecule is upregulated during differentiation.<sup>40</sup> To determine the percentage of positive cells, the viable cell population were gated for using the forward scattering and side scattering results (Fig. 1 and S1). The percentage of CD44<sup>+</sup>/CD24<sup>-</sup> cells were significantly lower in the MCF-7-mammospheres treated with silibinin compared with the respective control (Fig. 4A and 4B), and did not differ significantly in the other cell lines. The mean fluorescence intensity (MFI) of CD44<sup>+</sup> cells were significantly increased in treated MDA-MB-231 and MDA-MB-468 cells. However, the MFI of CD44 in MDA-MB-468 was not significant when dual staining was done with CD133. MFI of CD44 did not change in the MCF-7 cells before and after Silibinin treatment (Fig. 4C and S2). CD133 expression was not altered by treatment with silibinin in the MDA-MB-231 and MDA-MB-468 cells, whereas expression was significantly reduced in the MCF-7 mammospheres when treated (Fig. 4D-F).

#### **Silibinin reduces the invasive and migratory potential of mammospheres**

It has been hypothesized that CSCs potentiate invasion of cancer cells<sup>41</sup> Therefore, the effect of silibinin on invasion and migration of mammospheres was determined. As shown in Fig. 5, both the migratory and invasive capacity of mammospheres was reduced significantly following treatment with silibinin at the respective IC<sub>50</sub> doses. The number of cells which had invaded decreased 4.6 fold ( $P < 0.0008$ ) and the number cells which had migrated decreased 1.3-fold in the MCF-7 mammospheres (Fig. 5A), 4.2-fold decrease (invasion) and 2-fold decrease (migration) in the MDA-MB-231 mammospheres (Fig.

5B), and 2-fold decrease (invasion) and 3-fold decrease (migration) in MDA-MB-468 cells when treated with silibinin (Fig. 5C). Reduction of invasion and migration in MDA-MB-231 and MDA-MB-468 cells were associated with downregulation of EMT-associated genes (Fig. 5B and 5C). In MCF-7 mammospheres, several EMT-associated genes, including *SNAIL2* and *TWIST1/2* were upregulated when treated with silibinin, although the migratory and invasive capacity were decreased significantly (Fig. 5).

#### **Silibinin reduces tumor growth in vivo**

To determine the effect of silibinin *in vivo*, a BC mouse model was used. Treatment with silibinin significantly reduced tumor volume after 3 days (Fig. 6A) and tumor weight (Fig. 6B). H&E staining showed a notable reduction in proliferation in mice treated with both 10- and 20-fold doses of silibinin (Fig. 6C). The infiltration of polymorphonuclear cells, inflammation, and necrosis was also increased in the treated mice (Fig. 6C; Table 2). Furthermore, a notable reduction of  $\alpha$ -SMA staining of endothelial tubes was observed in the mice treated with silibinin (Fig. 6D), suggesting that angiogenesis was reduced.

#### **Silibinin interacts directly with genes which contribute to metastasis and indirectly to self-renewal transcription factors**

As shown in Fig. 7A, silibinin directly interacted with *ZEB1*, *SNAIL1*, *CDH1*, and *CTNBB1*, and indirectly interacted with a number of major nodes, including the majority of the self-renewal and EMT associated genes. The catenin family (*CTNN*) (cadherin-associated proteins) formed large nodes in the identified network (Fig. 7B).

#### **Discussion**

The aim of the present study was to determine whether silibinin, which reduces tumor viability, could target BC stem cells. In our previous study, it was demonstrated that silibinin exhibited anti-cancer effects by inhibiting the effects of anti-apoptotic genes, including Bcl-2 and Survivin,<sup>27</sup> reducing tumor volume in 3D cultures, reducing sphere formation, and reducing colony formation. However, the effects of silibinin on BC stem cells were unknown. Mammospheres were used in the present study as mammospheres are rich in CSCs,<sup>42-44</sup> and the presence of a rare population of CSCs was confirmed based on an immunophenotyping model using CD44, CD24, and CD133 antibodies. Based on our previous study using other cell lines and on other published studies,<sup>45,46</sup> cell surface markers cannot be used as the only criteria for proper characterization of CSCs. Spheroid culture conditions may be a more effective approach to enrich CSCs, rather than the use of cell surface markers.<sup>30,31</sup> Additionally, mammospheres were an appropriate model for the present study as they simulate the geometric, mechanical, and

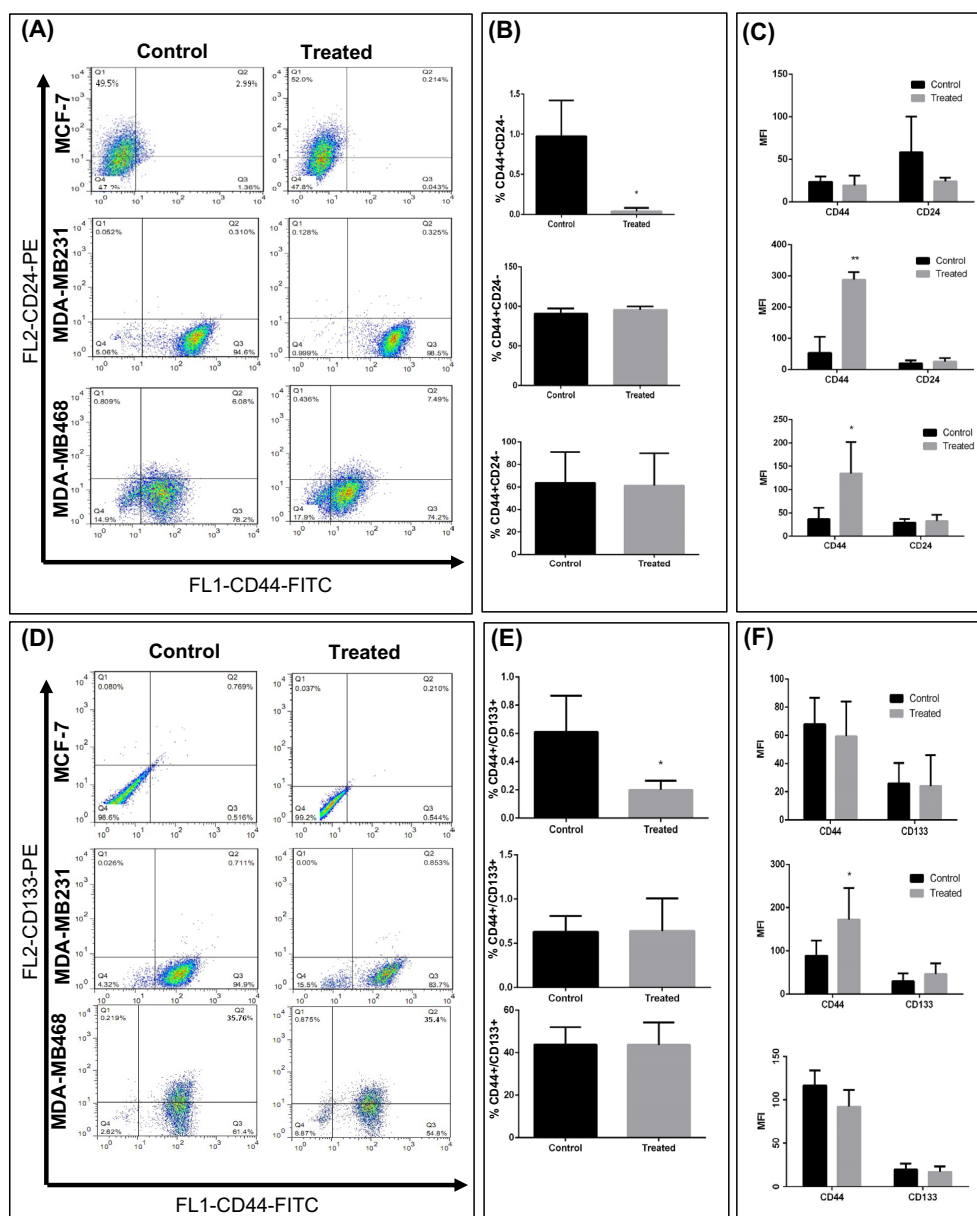


**Fig. 4.** Evaluation of breast cancer stem cell markers in mammosphere cells treated with silibinin. (A) Representative flow cytometry dot plots of CD24/CD44 stem cell markers in cells obtained from mammospheres. (B) Quantitative analysis of CD44/CD24 surface markers expression in treated and untreated mammospheres. A significant decrease was observed in CD44<sup>+</sup>/CD24<sup>-</sup> cells in treated MCF-7 cells. (C) MFI of CD44 and CD24 in each group. CD44 intensity increased in treated derived –mammospheres from MD-MB231 and MDA-MB-468 aggregated cells. (D) Representative flow cytometry dot plots of CD133/CD44 markers in cells obtained from mammospheres. (E) Quantitative analysis of CD133/CD44 surface markers expression in treated and untreated mammospheres. A significant decrease was observed in CD44<sup>+</sup>/CD133<sup>+</sup> cells in treated MCF-7 cells. (F) MFI of CD44 and CD133 in each group. CD44 intensity increased in treated MD-MB231 mammospheres. Data are presented as the mean  $\pm$  standard deviation of three biological repeats. \* $P < 0.05$ , \*\* $P < 0.01$  vs. control. MFI, mean fluorescence intensity; FITC, fluorescein isothiocyanate; PE, phycoerythrin., FL2, fluorescence parameter 2.

biochemical aspects of a tumor more accurately, and they better replicate cell-cell, and cell-substrate interactions, which in turn regulate proliferation and differentiation.<sup>30,31</sup> Mammospheres were derived from two different types of BC cell lines; MCF-7 (which were used as an ER<sup>+</sup>, PR<sup>+</sup> cell line), and MDA-MB-231 (which were both used as triple negative BC cell lines). Mammospheres were treated with silibinin and the effects of treatment on expression of stemness, differentiation-associated, and EMT associated genes, and migration and invasion were determined. The

IC<sub>50</sub> of silibinin for MCF-7-mammospheres was 150  $\mu$ M, for MDA-MB-231 was 100  $\mu$ M and for MDA-MB-468-mammospheres was 50  $\mu$ M. At the respective IC<sub>50</sub> doses, colony formation, sphere formation, and proliferation were all reduced, and the reduction was the largest in the MCF-7 cells. These results are consistent with our previous study,<sup>47</sup> and other reports in ovarian,<sup>18</sup> lung,<sup>45</sup> and colon cancer.<sup>46</sup> Treatment with silibinin reduced self-renewal potential, and this was associated with a reduction in mammosphere formation, proliferation, and

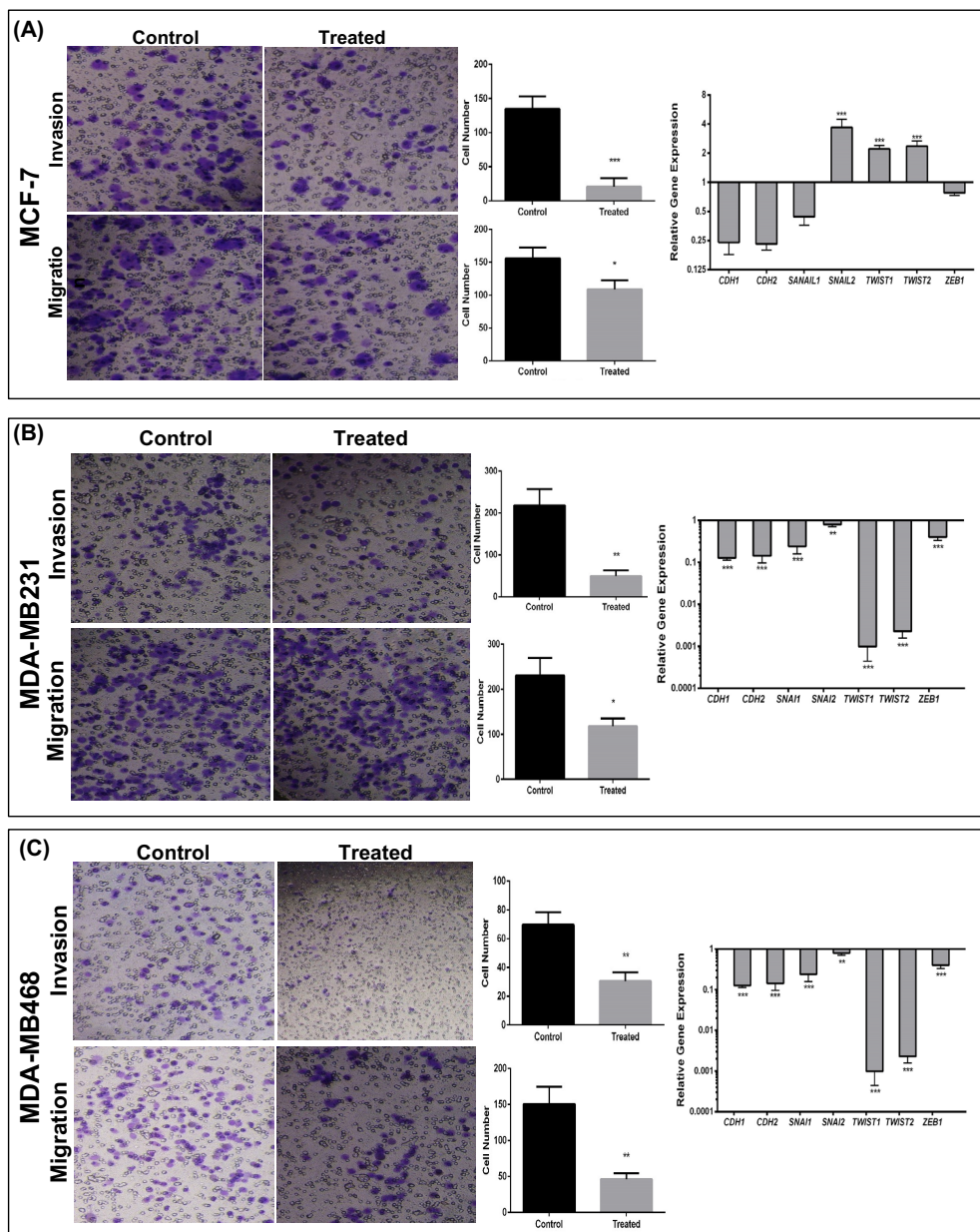


**Fig. 5.** Invasive and migratory capacity of silibinin-treated cells from mammospheres. (A-C) The migratory and invasive capacities of mammospheres were reduced in all silibinin-treated cells. These reductions were accompanied by downregulation of important transcription factors known to regulate metastasis in MDA-MB-231 and MDA-MB-468 cells, whereas treated MCF-7 cells exhibited upregulation of some transcription factors. (Left) Migrated and invaded cells visualized with crystal violet. (Center) Quantitative analysis of the number of migrated (upper) and invaded (lower) cells. (Right) Expression of epithelial-mesenchymal transition associated genes in treated compared with untreated mammospheres. Expression of genes was normalized to *GAPDH*. Data are presented as the mean ± standard deviation of three biological repeats. \**P*<0.05, \*\**P*<0.01, \*\*\**P*<0.001 vs. control.

**Table 2.** Histopathological analysis of tumor tissues in different groups

Group name	Mitosis per HPF	Pleomorphism	Inflammation	Karyorrhexis	Desmoplasia	Other
Control	6-7	2	Mild lymphocytic	Not determined	No	Lymph node involving fat
Solvent	6-7	2	Mild lymphocytic	Not determined	No	-
X 10	2-3 <sup>a</sup>	2	Moderate to severe lymph/PMN	+	No	Necrosis ++
X 20	2-3 <sup>a</sup>	2	Severe lymph/PMN	+	No	Necrosis +

<sup>a</sup>*P*<0.05. HPF, high power fields; PMN, polymorphonuclear neutrophils; Control, tumor bearing mice without any treatment; solvent, tumor bearing mice that received; X10, tumor bearing mice that received 1 mg/kg silibinin every 48 hours. X20, tumor bearing mice that received 2 mg/kg silibinin every 48 hours; +/++, quality observation.

colony formation. The proportion of CD44<sup>+</sup>/CD24<sup>-</sup> and CD44<sup>+</sup>/CD133<sup>+</sup> cells, which are considered CSCs in BC,<sup>48-50</sup> were reduced in the treated MCF-7-mammospheres. However, the expression of the majority of stemness-associated genes was downregulated in all cell lines assessed, and the expression of differentiation-associated genes (CK8, CK18, and CK19) were upregulated in MDA-MB-231 and MDA-MB-468 cells when treated with silibinin. Similar results have been reported in other types of cancer, including head and neck,<sup>51</sup> colon,<sup>25</sup>

nasopharyngeal carcinoma,<sup>52</sup> and colorectal cancer.<sup>53</sup> The expression of *c-MYC* and *NANOG/KLF4* was upregulated in treated derived -mammospheres from MCF-7 cells and MDA-MB-468 aggregation cells, respectively. *KLF-4* promotes or inhibits progression of cancer depending on the type of cancer and possibly other factors in the tumor microenvironment.<sup>53-55</sup> BC cell lines treated with silibinin exhibited upregulated expression of CK8, CK18, and CK19, suggesting that certain sub-populations of cancer cells may have undergone EMT.<sup>54-56</sup> Therefore,

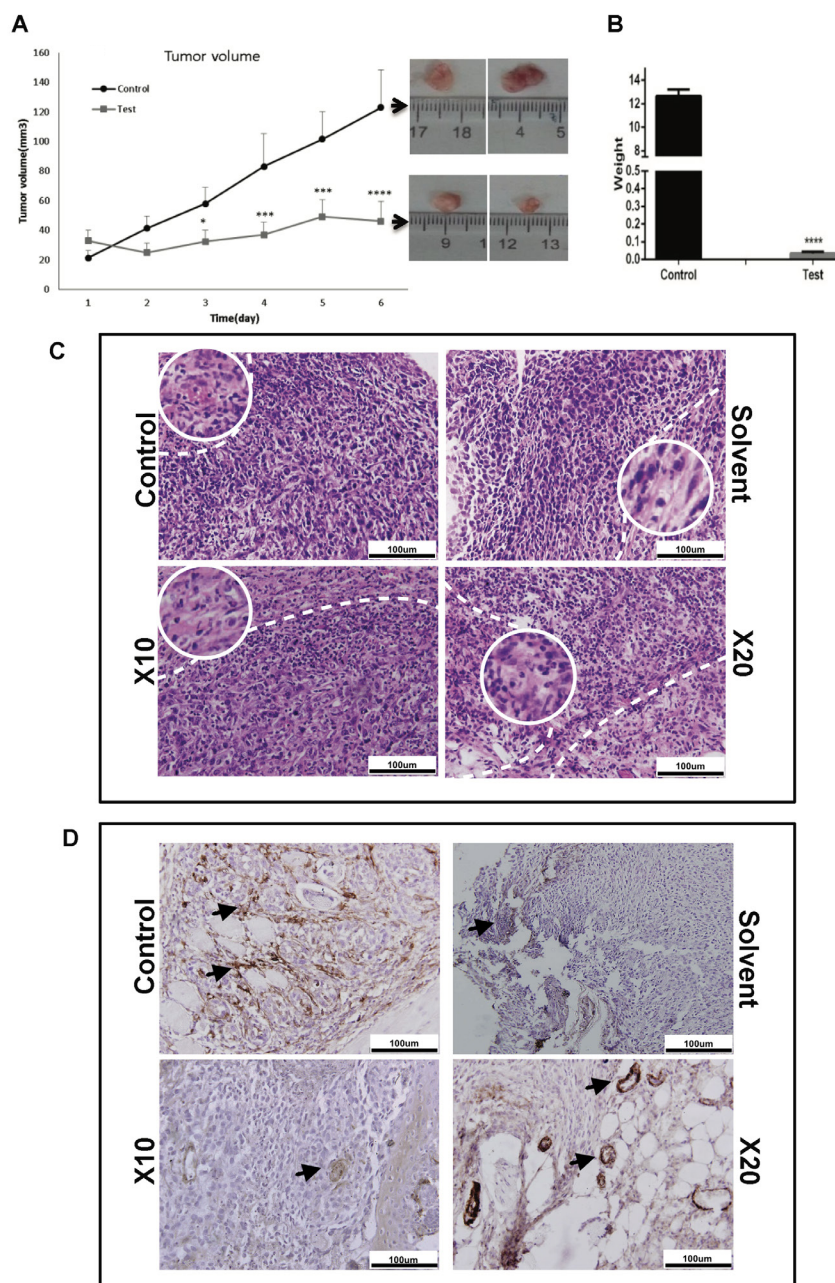


**Fig. 6.** The effect of silibinin on tumor growth in a breast cancer mouse model. Silibinin (2 mg/kg) was injected intra-tumor every 48 hours in mice exhibiting tumors with a 4-6 mm diameter. (A) Tumor volume and (B) weight were significantly reduced in treated mice compared with the untreated group. (C) Hematoxylin and eosin staining of tumors showed an apparent increase in the number of necrotic cells in the silibinin-treated group. Scale bar, 100  $\mu$ M (10X magnification). The white dash line showed necrotic area in each group and white circle indicated necrotic cell morphology in 20X-enlarged region. (D) Immunostaining for  $\alpha$ -SMA. Expression of  $\alpha$ -SMA (black arrows) was decreased in the tumors of treated mice. Scale bar, 100  $\mu$ M.

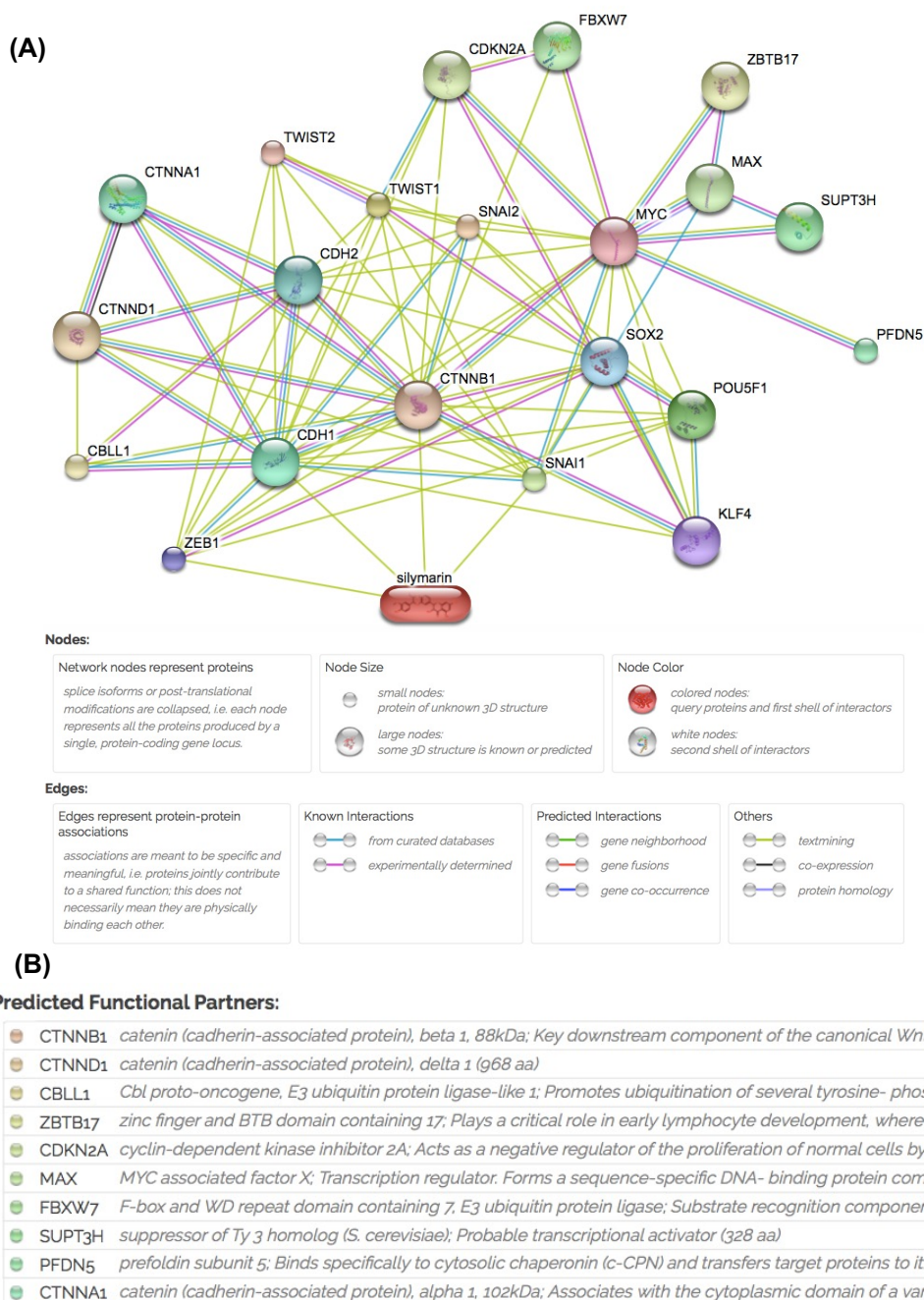


**Fig. 7.** Search Tool for Interactions of Chemicals analysis of silibinin interactions with proteins important in self-renewal and metastasis. (A) The network shows different nodes with various interactions between silibinin and associated genes including predicted interactions. (B) Predicted functional partner nodes and their function.

upregulation of these cytokeratins in the present study may inhibit micro-metastasis. The STAT3 signaling pathway serves as an important pathway in increasing proliferation and promoting the self-renewal capacity through *OCT4* or WNT signaling pathways in cancer.<sup>57,58</sup> Based on the results of the study, treatment with silibinin reduced the levels of phosphorylated STAT3 in MCF-7-mammospheres, although it is not certain whether the total levels of Stat3 were reduced. The decreased levels of phosphorylated STAT3 may underlie the reduction in

cell proliferation observed in treated cells. It has also been reported that silibinin may affect the expression of genes involved in drug resistance, including *AKT* and *ABCG2* through regulation of stemness factors<sup>19</sup> All alterations in cancer cell function were associated with a reduction in the tumorigenicity of BC cells in nude mice. Silibinin not only reduced proliferation and self-renewal *in vivo*, but also appeared to inhibit angiogenesis which has significant effects on tumor growth.  $\alpha$ -SMA expression analysis was performed to determine differences in angiogenesis.

## Research Highlights

### What is the current knowledge?

- ✓ Silibinin has anti-tumor effects on various cancers.
- ✓ Sphere-forming culture due to the availability of 3D culture is considered as a suitable alternative to animal models.
- ✓ Sphere-forming culture is a proper method to CSCs enrichment.

### What is new here?

- ✓ Silibinin can affect various CSCs.
- ✓ Anti-tumor effect of silibinin in breast cancer is related to direct targeting BCSCs.
- ✓ Silibinin can reduce the tumorigenicity and metastasis and promote differentiation in mammospheres.

One limitation of the present study was an inaccessibility to Ki67 and VEGF antibodies to confirm the results. The pattern of responses to silibinin in the two triple-negative BC cell lines were similar, and were both more sensitive to silibinin than the MCF-7 cells. The mechanism by which silibinin exhibits its effects are unknown, but it has been reported that silibinin inhibits progression of colorectal cancer stem-like cells through inhibition of the PP2A/AKT/mTOR signaling pathway,<sup>46</sup> as well as inhibiting the growth of colonospheres through the IL4/6 signaling pathway.<sup>25</sup> Furthermore, in human GBM, silibinin induced apoptosis and autophagy through simultaneous inhibition of the mTOR and YAP signaling pathways<sup>59</sup>; whereas in gastric cancer, silibinin reduced metastasis through the MAPK signaling pathway.<sup>60</sup>

In the present study, a reduction in the migratory and invasive capacity of mammospheres formed from all BC cell lines was demonstrated when treated with silibinin. The reduction in invasiveness may have been associated with downregulation of certain EMT-transcription factors in MDA-MB-231 and MDA-MB-468 cells. However, *SNAIL1* and *TWIST1/2* expressions were upregulated in treated MCF-7 cells, but the migratory and invasive capacity were still significantly decreased. Therefore, silibinin may control both stemness and metastatic potential, and the balance of transcription factors by an unknown regulatory network which may determine the fate of cancer cells. Use of the STITCH database identified that silibinin may have exerted its effect directly by regulation of metastasis-associated genes, particularly *ZEB1*, *SNAIL1*, *CDH1*, and *CTNBB1*. Therefore, it is hypothesized that the direct effects of silibinin on metastasis-associated genes, particularly *ZEB1*, *SNAIL1*, *CDH1*, and *CTNBB1*, and the indirect effects on stemness-associated genes may be the mechanism by which silibinin affected cell behaviors. Although no signs of metastasis were observed in the treated and control group *in vivo* (data not shown), an additional control in the *in vivo* experiments should be used in future experiments to determine the effect of

silibinin on metastasis in the mouse model.

## Conclusion

In conclusion, it was demonstrated that silibinin significantly decreased mammosphere and aggregated cells viability, colony and sphere formation, and migration and invasion. Furthermore, silibinin altered differentiation in BC cells, highlighting its potential as a therapeutic option for treatment of BC.

## Acknowledgments

The authors would like to thank Mr. Payam Taheri, Mr. Abolfazle Kheimeh and Mr. Shahab Mirshahvaladi (Royan Institute for Stem Cell Biology and Technology, ACECR, Tehran, Iran) for their technical assistance and helpful advice.

## Funding sources

The present study was funded by grants from Iran National Science Foundation (Grant no. 90003728) and Iranian Council of Stem Cell Research and Technology (Grant no. REP191).

## Ethical statement

All procedures in the present study were performed in accordance with the relevant guidelines and regulations of the Royan Institute for Stem Cell Biology and Technology and approved by the Institutional Review Board and Ethics Committee of the Royan Institute, Tehran, Iran (approval no. IR.ACECR.ROYAN.REC.1395.35).

## Competing interests

The authors declare that they have no competing interests.

## Authors' contribution

JF contributed to the conceptualization of the study, and data collection, and was a major contributor to writing the manuscript. AS, MR, PS, MA, and EJ contributed to data collection and data analysis. FS revised the manuscript and supervised the study. NS contributed to the pathological analysis. MS contributed to writing and editing the manuscript. ME contributed to the conceptualization of the study, revised the manuscript, and supervised the study. All authors read and approved the final manuscript.

## Data availability statement

The data that support the findings of this study are available from the corresponding author upon reasonable request.

## Supplementary Materials

Supplementary file 1 contains Figs. S1-S2.

## References

1. Ferlay J, Soerjomataram I, Dikshit R, Eser S, Mathers C, Rebelo M, *et al.* Cancer incidence and mortality worldwide: sources, methods and major patterns in GLOBOCAN 2012. *Int J Cancer* **2015**; 136: E359-E86. <https://doi.org/10.1002/ijc.29210>
2. Keller PJ, Arendt LM, Skibinski A, Logvinenko T, Klebba I, Dong S, *et al.* Defining the cellular precursors to human breast cancer. *Proc Natl Acad Sci U S A* **2012**; 109: 2772-7. <https://doi.org/10.1073/pnas.1017626108>
3. Vinogradov S, Wei XJN. Cancer stem cells and drug resistance: the potential of nanomedicine. *Nanomedicine (Lond)* **2012**; 7: 597-615. <https://doi.org/10.2217/nmm.12.22>
4. Chen K, Huang Y-h, Chen J-IJAPS. Understanding and targeting cancer stem cells: therapeutic implications and challenges. *Acta Pharmacol Sin* **2013**; 34: 732-40. <https://doi.org/10.1038/aps.2013.27>
5. Han L, Shi S, Gong T, Zhang Z, Sun XJAPSB. Cancer stem cells: therapeutic implications and perspectives in cancer therapy. *Acta Pharmaceutica Sinica B* **2013**; 3: 65-75. <https://doi.org/10.1016/j.apsb.2013.02.006>

6. Reynolds DS, Tevis KM, Blessing WA, Colson YL, Zaman MH, Grinstaff MWJSr. Breast cancer spheroids reveal a differential cancer stem cell response to chemotherapeutic treatment. *Sci Rep* **2017**; 7: 1-12. <https://doi.org/10.1038/s41598-017-10863-4>
7. Aggarwal BB, Danda D, Gupta S, Gehlot PJBp. Models for prevention and treatment of cancer: problems vs promises. *Biochem Pharmacol* **2009**; 78: 1083-94. <https://doi.org/10.1016/j.bcp.2009.05.027>
8. Friedrich J, Eder W, Castaneda J, Doss M, Huber E, Ebner R, et al. A reliable tool to determine cell viability in complex 3-d culture: the acid phosphatase assay. *J Biomol Screen* **2007**; 12: 925-37. <https://doi.org/10.1177/1087057107306839>
9. Abbott A. Biology's new dimension. *Nature* **2003**; 424: 870-2. <https://doi.org/10.1038/424870a>
10. Zhu X-X, Ding Y-H, Wu Y, Qian L-Y, Zou H, He QJErcep. Silibinin: a potential old drug for cancer therapy. *Expert Rev Clin Pharmacol* **2016**; 9: 1323-30. <https://doi.org/10.1080/17512433.2016.1208563>
11. Kaur M, Velmurugan B, Tyagi A, Deep G, Katiyar S, Agarwal C, et al. Silibinin suppresses growth and induces apoptotic death of human colorectal carcinoma LoVo cells in culture and tumor xenograft. *Mol Cancer Ther* **2009**; 8: 2366-74. <https://doi.org/10.1158/1535-7163.MCT-09-0304>
12. Zhang X, Liu J, Zhang P, Dai L, Wu Z, Wang L, et al. Silibinin induces G1 arrest, apoptosis and JNK/SAPK upregulation in SW1990 human pancreatic cancer cells. *Oncol Lett* **2018**; 15: 9868-76. <https://doi.org/10.3892/ol.2018.8541>
13. Deep G, Singh R, Agarwal C, Kroll D, Agarwal RJO. Silymarin and silibinin cause G1 and G2-M cell cycle arrest via distinct circuitries in human prostate cancer PC3 cells: a comparison of flavanone silibinin with flavanolignan mixture silymarin. *Oncogene* **2006**; 25: 1053-69. <https://doi.org/10.1038/sj.onc.1209146>
14. Surai PFJA. Silymarin as a natural antioxidant: an overview of the current evidence and perspectives. *Antioxidants (Basel)* **2015**; 4: 204-47. <https://doi.org/10.3390/antiox4010204>
15. Yang S-H, Lin J-K, Chen W-S, Chiu J-HJJoSR. Anti-angiogenic effect of silymarin on colon cancer LoVo cell line. *J Surg Res* **2003**; 113: 133-8. [https://doi.org/10.1016/s0022-4804\(03\)00229-4](https://doi.org/10.1016/s0022-4804(03)00229-4)
16. Loguercio C, Festi DJWjogW. Silybin and the liver: from basic research to clinical practice. *World J Gastroenterol* **2011**; 17: 2288. <https://doi.org/10.3748/wjg.v17.i18.2288>
17. Ramasamy K, Agarwal RJCl. Multitargeted therapy of cancer by silymarin. *Cancer Lett* **2008**; 269: 352-62. <https://doi.org/10.1016/j.canlet.2008.03.053>
18. Momeny M, Ghasemi R, Valenti G, Miranda M, Zekri A, Zarrinrad G, et al. Effects of silibinin on growth and invasive properties of human ovarian carcinoma cells through suppression of heregulin/HER3 pathway. *Tumour Biol* **2016**; 37: 3913-23. <https://doi.org/10.1007/s13277-015-4220-6>
19. Deep G, Agarwal RJC, Reviews M. Antimetastatic efficacy of silibinin: molecular mechanisms and therapeutic potential against cancer. *Cancer Metastasis Rev* **2010**; 29: 447-63. <https://doi.org/10.1007/s10555-010-9237-0>
20. Liakopoulou C, Kazakis C, Vallianou NGJA-CAiMC. Silimarin and Cancer. *Anticancer Agents Med Chem* **2018**; 18: 1970-4. <https://doi.org/10.2174/1871520618666180905154949>
21. Chatran M, Pilehvar-Soltanahmadi Y, Dadashpour M, Faramarzi L, Rasouli S, Jafari-Gharabaghloou D, et al. Synergistic anti-proliferative effects of metformin and silibinin combination on T47D breast cancer cells via hTERT and cyclin D1 inhibition. *Drug Res (Stuttg)* **2018**; 68: 710-6. <https://doi.org/10.1055/a-0631-8046>
22. Zhang Y, Ge Y, Ping X, Yu M, Lou D, Shi WJmMr. Synergistic apoptotic effects of silibinin in enhancing paclitaxel toxicity in human gastric cancer cell lines. *Mol Med Rep* **2018**; 18: 1835-41. <https://doi.org/10.3892/mmr.2018.9129>
23. Wu K, Ning Z, Zeng J, Fan J, Zhou J, Zhang T, et al. Silibinin inhibits  $\beta$ -catenin/ZEB1 signaling and suppresses bladder cancer metastasis via dual-blocking epithelial-mesenchymal transition and stemness. *Cell Signal* **2013**; 25: 2625-33. <https://doi.org/10.1016/j.cellsig.2013.08.028>
24. Alimoghaddam K, Ghavamzadeh AJAoIm. Silibinin induces apoptosis and inhibits proliferation of estrogen receptor (ER)-negative breast carcinoma cells through suppression of nuclear factor kappa B activation. *Arch Iran Med* **2014**; 17: 366.
25. Kumar S, Raina K, Agarwal C, Agarwal RJO. Silibinin strongly inhibits the growth kinetics of colon cancer stem cell-enriched spheroids by modulating interleukin 4/6-mediated survival signals. *Oncotarget* **2014**; 5: 4972. <https://doi.org/10.18632/oncotarget.2068>
26. Mao J, Yang H, Cui T, Pan P, Kabir N, Chen D, et al. Combined treatment with sorafenib and silibinin synergistically targets both HCC cells and cancer stem cells by enhanced inhibition of the phosphorylation of STAT3/ERK/AKT. *Eur J Pharmacol* **2018**; 832: 39-49. <https://doi.org/10.1016/j.ejphar.2018.05.027>
27. Abdollahi P, Ebrahimi M, Motamed N, Samani FSJA-cd. Silibinin affects tumor cell growth because of reduction of stemness properties and induction of apoptosis in 2D and 3D models of MDA-MB-468. **2015**; 26: 487-97.
28. Friedrich J, Seidel C, Ebner R, Kunz-Schughart LAJNp. Spheroid-based drug screen: considerations and practical approach. *Nat Protoc* **2009**; 4: 309. <https://doi.org/10.1038/nprot.2008.226>
29. Livak KJ, Schmittgen TDJm. Analysis of relative gene expression data using real-time quantitative PCR and the 2- $\Delta\Delta$ CT method. *Methods* **2001**; 25: 402-8. <https://doi.org/10.1006/meth.2001.1262>
30. Fomeshi MR, Ebrahimi M, Mowla SJ, Firouzi J, Khosravani PJcJ. CD133 is not suitable marker for isolating melanoma stem cells from D10 cell line. *Cell J* **2016**; 18: 21. <https://doi.org/10.22074/cellj.2016.3983>
31. Roudi R, Madjd Z, Ebrahimi M, Samani FS, Samadikuchaksaraei AJC, letters mb. CD44 and CD24 cannot act as cancer stem cell markers in human lung adenocarcinoma cell line A549. *Cell Mol Biol Lett* **2014**; 19: 23. <https://doi.org/10.2478/s11658-013-0112-1>
32. Segatto I, Baldassarre G, Belletti BJlJoms. STAT3 in breast cancer onset and progression: a matter of time and context. *Int J Mol Sci* **2018**; 19: 2818. <https://doi.org/10.3390/ijms19092818>
33. Galoczova M, Coates P, Vojtesek BJC, letters mb. STAT3, stem cells, cancer stem cells and p63. *Cell Mol Biol Lett* **2018**; 23: 12. <https://doi.org/10.1186/s11658-018-0078-0>
34. Chung SS, Aroh C, Vadgama JVPo. Constitutive activation of STAT3 signaling regulates hTERT and promotes stem cell-like traits in human breast cancer cells. *PLoS One* **2013**; 8. <https://doi.org/10.1371/journal.pone.0083971>
35. Al-Hajj M, Wicha MS, Benito-Hernandez A, Morrison SJ, Clarke MFJPotNAoS. Prospective identification of tumorigenic breast cancer cells. *Proc Natl Acad Sci U S A* **2003**; 100: 3983-8. <https://doi.org/10.1073/pnas.0530291100>
36. Wu Y, Wu PYJSc, development. CD133 as a marker for cancer stem cells: progresses and concerns. *Stem Cells Dev* **2009**; 18: 1127-34. <https://doi.org/10.1089/scd.2008.0338>
37. Sahlberg SH, Spiegelberg D, Glimelius B, Stenerlöv B, Nestor MJPo. Evaluation of cancer stem cell markers CD133, CD44, CD24: association with AKT isoforms and radiation resistance in colon cancer cells. *PLoS One* **2014**; 9. <https://doi.org/10.1371/journal.pone.0094621>
38. Shipitsin M, Campbell LL, Argani P, Weremowicz S, Bloushtain-Qimron N, Yao J, et al. Molecular definition of breast tumor heterogeneity. *Cancer Cell* **2007**; 11: 259-73. <https://doi.org/10.1016/j.ccr.2007.01.013>
39. Götte M, Yip GWJCr. Heparanase, hyaluronan, and CD44 in cancers: a breast carcinoma perspective. *Cancer Res* **2006**; 66: 10233-7. <https://doi.org/10.1158/0008-5472.CAN-06-1464>
40. Jaggupilli A, Elkord EJC, Immunology D. Significance of CD44 and CD24 as cancer stem cell markers: an enduring ambiguity. *Journal of Immunology Research* **2012**; 2012. <https://doi.org/10.1155/2012/708036>
41. Ayob AZ, Ramasamy TSJJobs. Cancer stem cells as key drivers of tumour progression. *J Biomed Sci* **2018**; 25: 20. <https://doi.org/10.1186/s12929-018-0426-4>
42. Zhou J. MCF7 side population cells and sphere culture as models for breast cancer stem-like cell biology and drug identification.

- cancerres **2008**. <https://doi.org/10.1158/0008-5472.CAN-07-2249>
43. de la Mare J-A, Sterrenberg JN, Sukhthankar MG, Chiwakata MT, Beukes DR, Blatch GL, *et al*. Assessment of potential anti-cancer stem cell activity of marine algal compounds using an in vitro mammosphere assay. *Cancer Cell Int* **2013**; 13: 39. <https://doi.org/10.1186/1475-2867-13-39>
  44. Wang R, Lv Q, Meng W, Tan Q, Zhang S, Mo X, *et al*. Comparison of mammosphere formation from breast cancer cell lines and primary breast tumors. *J Thorac Dis* **2014**; 6: 829. <https://doi.org/10.3978/j.issn.2072-1439.2014.03.38>
  45. Maiuthed A, Chantarawong W, Chanvorachote PJA. Lung cancer stem cells and cancer stem cell-targeting natural compounds. *Anticancer Res* **2018**; 38: 3797-809. <https://doi.org/10.21873/anticancer.12663>
  46. Wang JY, Chang CC, Chiang CC, Chen WM, Hung SCJ. Silibinin suppresses the maintenance of colorectal cancer stem-like cells by inhibiting PP2A/AKT/mTOR pathways. *J Cell Biochem* **2012**; 113: 1733-43. <https://doi.org/10.1002/jcb.24043>
  47. Abdollahi P, Ebrahimi M, Motamed N, Samani FSJA-cd. Silibinin affects tumor cell growth because of reduction of stemness properties and induction of apoptosis in 2D and 3D models of MDA-MB-468. *Anticancer Drugs* **2015**; 26: 487-97.
  48. Al-Hajj M, Wicha MS, Benito-Hernandez A, Morrison SJ, Clarke MFJPotNAoS. Prospective identification of tumorigenic breast cancer cells. **2003**; 100: 3983-8.
  49. de Beça FF, Caetano P, Gerhard R, Alvarenga CA, Gomes M, Paredes J, *et al*. Cancer stem cells markers CD44, CD24 and ALDH1 in breast cancer special histological types. *J Clin Pathol* **2013**; 66: 187-91. <https://doi.org/10.1136/jclinpath-2012-201169>
  50. Tume L, Paco K, Ubidia-Incio R, Moya JJGMdO. CD133 in breast cancer cells and in breast cancer stem cells as another target for immunotherapy. *Gaceta Mexicana de Oncología* **2016**; 15: 22-30. <https://doi.org/10.1016/j.gamo.2016.01.003>
  51. Chang Y-C, Jan C-I, Peng C-Y, Lai Y-C, Hu F-W, Yu C-CJO. Activation of microRNA-494-targeting Bmi1 and ADAM10 by silibinin ablates cancer stemness and predicts favourable prognostic value in head and neck squamous cell carcinomas. *Oncotarget* **2015**; 6: 24002. <https://doi.org/10.18632/oncotarget.4365>
  52. Luo W, Li S, Peng B, Ye Y, Deng X, Yao KJ. Embryonic stem cells markers SOX2, OCT4 and Nanog expression and their correlations with epithelial-mesenchymal transition in nasopharyngeal carcinoma. *PLoS One* **2013**; 8. <https://doi.org/10.1371/journal.pone.0056324>
  53. Raina K, Kumar S, Dhar D, Agarwal R. Silibinin and colorectal cancer chemoprevention: a comprehensive review on mechanisms and efficacy. *J Biomed Res* **2016**; 30: 452. <https://doi.org/10.7555/JBR.30.20150111>
  54. Weissenstein U, Schumann A, Reif M, Link S, Toffol-Schmidt UD, Heusser P. Detection of circulating tumor cells in blood of metastatic breast cancer patients using a combination of cytokeratin and EpCAM antibodies. *BMC Cancer* **2012**; 12: 206. <https://doi.org/10.1186/1471-2407-12-206>
  55. Gusterson BA, Ross DT, Heath VJ, Stein T. Basal cytokeratins and their relationship to the cellular origin and functional classification of breast cancer. *Breast Cancer Res* **2005**; 7: 143. <https://doi.org/10.1186/bcr1041>
  56. Malzahn K, Mitze M, Thoenes M, Moll R. Biological and prognostic significance of stratified epithelial cytokeratins in infiltrating ductal breast carcinomas. *Virchows Arch* **1998**; 433: 119-29. <https://doi.org/10.1007/s004280050226>
  57. Ye S, Liu D, Ying Q-L. Signaling pathways in induced naive pluripotency. *Curr Opin Genet Dev* **2014**; 28: 10-5. <https://doi.org/10.1016/j.gde.2014.08.002>
  58. Wei D, Kanai M, Huang S, Xie K. Emerging role of KLF4 in human gastrointestinal cancer. *Carcinogenesis* **2005**; 27: 23-31. <https://doi.org/10.1093/carcin/bgi243>
  59. Bai Z-L, Tay V, Guo S-Z, Ren J, Shu M-G. Silibinin induced human glioblastoma cell apoptosis concomitant with autophagy through simultaneous inhibition of mTOR and YAP. *Biomed Res Int* **2018**; 2018. <https://doi.org/10.1155/2018/6165192>
  60. Kim S, Choi MG, Lee HS, Lee SK, Kim SH, Kim WW, *et al*. Silibinin suppresses TNF- $\alpha$ -induced MMP-9 expression in gastric cancer cells through inhibition of the MAPK pathway. *Molecules* **2009**; 14: 4300-11. <https://doi.org/10.3390/molecules14114300>